Investigating MALDI MSI parameters (Part 2) - On the use of a mechanically shuttered trigger system for improved laser energy stability

Steven, Rory T; Dexter, Alexander; Bunch, Josephine

DOI:
10.1016/j.ymeth.2016.04.013

Document Version
Peer reviewed version

Citation for published version (Harvard):
Steven, RT, Dexter, A & Bunch, J 2016, 'Investigating MALDI MSI parameters (Part 2) - On the use of a mechanically shuttered trigger system for improved laser energy stability', *Methods*, vol. 104, pp. 111-7. https://doi.org/10.1016/j.ymeth.2016.04.013

On the use of a mechanically shuttered trigger system for improved laser energy stability within MALDI MSI

Rory T. Steven[†], Alex Dexter[†,$], Josephine Bunch[†, ‡, *]

[†]: National Centre of Excellence in Mass Spectrometry Imaging (NiCE-MSI), National Physical Laboratory (NPL), Teddington, UK, TW11 0LW

[$]: University of Birmingham, School of Chemistry, B15 2TT

[‡]: School of Pharmacy, University of Nottingham, NG7 2RD

*: Corresponding author: josephine.bunch@npl.co.uk

Abstract

Matrix assisted laser desorption ionization mass spectrometry imaging (MALDI MSI) is now widely used to desorb, ionize and detect molecules from complex samples and tissue sections. The detected ion intensity within MALDI MS and MSI is intimately linked to the laser energy-per-pulse incident upon the sample during analysis. Laser energy / power stability can be significantly affected by the manner in which the laser is operated. Higher repetition rate diode-pumped solid-state (DPSS) lasers are being increasingly adopted to enable high-throughput MALDI MSI analysis. Within this work two different laser triggering setups are used to demonstrate the effect of laser energy instabilities due to spiking and thermal control phenomena and a shutter triggering setup designed to remove these effects. The effect of non-equilibrium operation on MALDI MSI data versus the more stable energy of the shutter triggered system is demonstrated in thin films of α-cyano-4-hydroxycinnamic acid (CHCA) and for imaging of murine brain tissue sections. Significant unwanted variation in absolute and relative detected ion intensity are shown where energy variation is introduced by these phenomena; these return to equilibrium, within the setup employed here, over timescales which are very relevant to MALDI MS analysis.

Introduction

The intensity of detected ions within matrix assisted laser desorption ionisation mass spectrometry (MALDI MS) is intimately linked to the incident number of laser photons per unit area on the sample. This relationship is typically described by the power law relationship $I \propto H^m$ where I is the detected ion intensity, H is the fluence and m is the fitting parameter.[1] Consequently, fluctuations in incident laser energy may have a large effect on the detected ion intensity, potentially giving a false value for the sample being analysed or introducing a larger variation in the detected number of ions than may be desired. The energy output of a laser can vary for a number of reasons including: long term depletion due to damage of optical components, short time scale high energy pulses due to spiking and wandering behaviours due to thermal control and equilibration of the laser and / or the room in which the laser is housed. Potentially significant causes of energy variation within MALDI MS experimentation, where the laser needs to be repeatedly triggered for relatively short time periods (i.e. for the ablation of material from a pixel or row of pixels), are spiking and the thermal equilibration of the lasing components during those intermittent periods of triggering. Spiking is caused when resonator losses are suddenly reduced after some time of extended pumping of the gain medium, such as Q-switching, causing a series of high energy pulses to be emitted prior to the lasing process reaching a steady-state and the energy-per-pulse stabilising. Spiking is commonly observed within laser systems in which the upper state lifetime is much larger than the cavity damping time, i.e. if the time period between triggered laser pulses is shorter than the upper state lifetime of the gain medium, as is common in some high repetition rate DPSS lasers used in MALDI MSI. One way to ensure

steady state, equilibrium-operation of a laser within a system such as a MALDI mass spectrometer is to continuously trigger the laser at the desired repetition rate to ensure steady-state operation. Then, during analysis, turn the laser 'on' and 'off' by opening and closing a mechanical shutter placed in the path of the beam.

Laser based systems in fields other than MALDI MS have utilised shutter systems to minimise laser energy variability due to spiking and other non-equilibrium energy variations as well as to allow greater control over pulse timing. Shutters have been used in femtosecond laser desorption and ionisation setups to better control the timing of laser pulses arriving at the sample [2, 3]. A shutter systems was used by Bradshaw *et al.* within their combined laser desorption ionisation (LDI) and atomic force microscopy (AFM) system to enable laser control for desired pulse timing. [4] In laser ablation inductively couple plasma mass spectrometry (LA-ICP-MS) it is considered good practice to include a shutter system to remove pulse to pulse variability, as well as inclusion of an energy meter to monitor the delivery as it occurs[5].

Shutter systems have been used explicitly on a few occasions within the field of MALDI MS and MSI. Zavalin *et al.* allowed single laser shots to be transmitted to their sample for analysis at a rate of 100 Hz for transmission mode MALDI MS imaging [6]. Westmacott *et al.* made use of a mechanical shutter system to improve pulse-to-pulse stability of their laser in fundamentals studies of the influence of laser fluence in MALDI MS [7]. No data, however, in either of these examples, was presented on the effect of these shutter systems on the MADLI MS data obtained.

The intimate link between detected ion intensity and laser energy coupled with the clear need in all analytical techniques to reduce instrument induced variance within the data

demonstrates the need to inform researchers of the effects of laser instability and its mitigation by the use of shutters. Particularly within a field where modification of existing and building of new ion sources and their accompanying laser optics is relatively common.

Within this study we demonstrate the presence of energy spiking phenomena in a MALDI MS relevant triggering setup. The mitigation of this effect under the same analytical conditions is then demonstrated. Data is acquired under both of these setups in thin film α-cyano-4-hydroxycinnamic acid (CHCA) and in CHCA coated murine brain tissue imaging by MALDI MSI. Multivariate analyses are also implemented to further probe the spectral differences resulting from MALDI MSI analyses under these two triggering regimes.

Methods

Materials

Methanol (HPLC grade) was purchased from Fisher Scientific (Leicestershire, UK). Water was purified by an ELGA Purelab Option system (Marlow, UK). Trifluoroacetic acid (TFA, 99.9 % purity) and MALDI matrix α-cyano-4-hydroxycinnamic acid (CHCA) were purchased from Sigma Aldrich (Dorset, UK). MALDI MS stainless steel imaging plates from Sciex (Ontario, Canada) were used for all samples.

Tissue Preparation and Sectioning

Mice were sacrificed humanly at the School of Cancer Sciences, University of Birmingham in accordance with the Home Office Animals (Scientific Procedures) Act 1986 [8]. Mouse brain was flash frozen in liquid nitrogen immediately after excision. 2 serial sections at 10 µm thick

were collected and thaw mounted onto a single MALDI imaging plate (Sciex). Sectioning was performed on a CM 1850 Cryo-microtome (Leica, Milton Keynes, UK).

Matrix Application

For the thin film and tissue experiments CHCA (5 mg mL^{-1} in 80 % CH_3OH, 0.1 % TFA) was deposited onto the sample plate (plane MALDI imaging plate, Sciex) by TM Sprayer (HTX Technologies, Carrboro, NC) at a nebuliser temperature of 90 ^{o}C, a solvent flow rate of 0.115 mL/min, a gas pressure of 10 psi, and a nebuliser speed of 1333 mm min^{-1}. Eight sequential passes across the whole plate were used, each with a track spacing of 3 mm, an offset of 1.5 mm was applied on every other pass with alternating horizontal and vertical path direction. This gave a density of matrix on the plate of 0.115 mg cm^{-2}.

Mass Spectrometry

MALDI TOF MS analysis was carried out on a QSTAR XL QqTOF instrument using Analyst QS 1.1 with oMALDI server 5.1 (Sciex, Warrington, UK). An Nd:YAG (Elforlight, Daventry, UK:FQS-100-1-Y-355) DPSS laser with $\lambda = 355$ nm, ≤ 10 kHz repetition rate and < 4 ns pulse length was used in this study. In all cases the laser was triggered directly from a function generator (TTi – TG2000 20MHz DDS). For the shutter triggered data acquisition the QSTAR oMALDI software controlled trigger signal was coupled to a shutter (2.5 cm diaphragm shutter, 10 ms full aperture opening time, Thorlabs Ltd, Ely, UK) which was placed in the path of the laser beam prior to fibre coupling (see Figure 1 for schematic optics setup used within this study). Therefore, the laser remained on continuously whilst the shutter, as triggered by the QSTAR software, allowed or prevented the laser ablation on the sample itself. For the non-shutter

controlled sample analysis the shutter was set continuously to open and the function generator was triggered directly from the QSTAR instead. All MALDI MSI analyses were carried out in continuous raster mode. Consequently, the laser is triggering is initiated (by either method) at the beginning of each raster line and it fires continuously until the end of the raster line when the triggering ceases. Therefore, the shutter is opened (or pulse generator begins its pulse train) at the start of each raster line and is closed (pulse train is stopped) at the end of each raster line.

The laser was coupled to the MALDI source via a 100 µm core diameter fibre optic patchcord (4 meters, Fiberguide Industries via AMS Technologies, Leicestershire, UK, NA = 0.22). The raster speed used were dictated by the preset speed values available within the oMALDI (Sciex) software and the slower speed corresponding to 0.3 mm/s was used within this study. An *m/z* range of 50 – 1000 was used for all experiments. All data were acquired in positive ion mode.

For the CHCA thin film analysis the Nd:YAG laser was operated at 3.3 kHz at a raster speed of 0.3 mm/s (named slower in the oMALDI software). Laser energies used are displayed within the main body of this article. Four raster lines of 126 pixels (each 100 µm wide) in length was acquired for each variable combination in continuous stage raster imaging mode.

Tissue image data were acquired at stage speeds of 0.3 mm/s at repetition rates of 4 kHz. The same half of each coronal section was analysed. These images were acquired with pixel sizes of 100 x 100 µm and took approximately 20 minutes to acquire per image.

Laser Beam Profiling and Energy Measurement

The irradiated area on the sample as measured by the fluorometric method utilising the fluorescence from CHCA at low (non-ablating) energies [9] was 2.05×10^{-8} m^2. The laser energy per pulse was measured using a pyro-electric sensor (PD10-C, Ophir Photonics) both post fibre and from the beam sampler prior to the experiment and from the beam sampler during the experiment allowing the energy incident to be calculated from this calibration. A Watt Pilot (Altechna, Lithuania) computer controlled half wave plate and Brewster angle filter attenuation setup was used to attenuate the beam post laser. A schematic of the laser delivery setup are shown in the supplementary information Figure 1.

Processing of MALDI MSI Data

The data was converted from AB Sciex proprietary file format (.wiff) to .mzML using AB MS Data Converter (Sciex, version 1.3) and then converted to imzML using imzMLConverter. [10] Further processing was carried out on in-house software running from MatLab (version R2014b, Math Works Inc, USA). The mean ion counts (peak area) for selected mass-to-charge values were calculated along with the standard deviation and are plotted as mean value ± s.d. The image colour scheme was chosen to align with mass spectrometric best practice guidelines.[11] Multivariate analyses (MVA) were carried out with the following pre-processing: zero filling, 3 sequential Savitzky-Golay smoothing, window size 7, polynomial order 2, negatives removed, TIC normalised where stated, gradient peak picked with top 2000 peaks retained for multivariate analyses. PCA was carried out according to the memory efficient method [12] and non-negative matrix factorisation (NMF) by using the MATLAB function nnmf with k = 5.

Results and Discussion

On laser stability in MALDI MS and MSI relevant laser systems

Triggering of the laser within the setup employed for these studies (and other studies with similarly triggered laser systems within MALDI MS and MSI) involves the active release of the 1062 nm photons from the diode pumped lasing medium. These photons go on to pass through the frequency doubling and tripling portions of the laser prior to exiting the laser. During MALDI MS analysis the lasing media and associated optics, if repeatedly triggered at the same frequency, the will operate at an equilibrium state where the emitted 355 nm photons exhibit optimal energy / power stability. However, within MALDI MS and MSI type experiments the laser triggering will typically only occur in this fashion for a short time during the analysis of each pixel or row of pixels. Outside of this time the primary lasing medium will still typically be pumped and lasing but the downstream optics may not be active. There are a number of issues related to this repeated pausing of triggering: the thermal stability of downstream optic elements of the laser are only ever approaching an equilibrium state and spiking may occur at the beginning of each pixel or raster line whereby a number of higher energy pulses are emitted until a steady-state is reached. Spiking results from the sudden reduction in resonator loss (triggered Q-switching of the laser for example) after a suitably long time where the gain medium was pumped. This may be particularly if the trigger frequency (repetition rate) provides only a short pump time between switching in comparison to the upper-state lifetime of the lasing media. Thus, the stored energy prior to triggering may be large compared to that emitted during continuous triggering (normal continuous operation).

The continuous variation between constant triggering and no triggering within MALDI MS experiments can, therefore, lend itself to the consistent presence of these potentially deleterious phenomena, the result of which may be seen with the detected mass spectra themselves due to the well-known relationship between laser energy and detected ion intensity within MALDI MS.[13]

Investigation into the use of a mechanical shutter in MALDI MSI of a thin matrix film

In order to investigate the effect of continuous laser operation with shutter triggering versus the direct triggering of the laser the optics setup coupling the laser to the QSTAR instrument was modified slightly to enable manual switching between these modes (Figure 1).

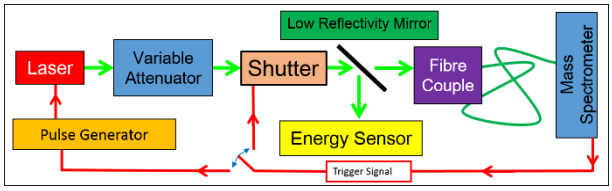

Figure 1. Schematic of optics setup used within these studies.

In initial investigation into the effect on MALDI MS derived spectra were carried out in thin films of CHCA matrix. Continuous raster mode image data was acquired at a fixed attenuation whilst simultaneously recording the laser energy from the beam sampling mirror to provide on-line energy measurement. Data from these analyses are presented within Figure 2.

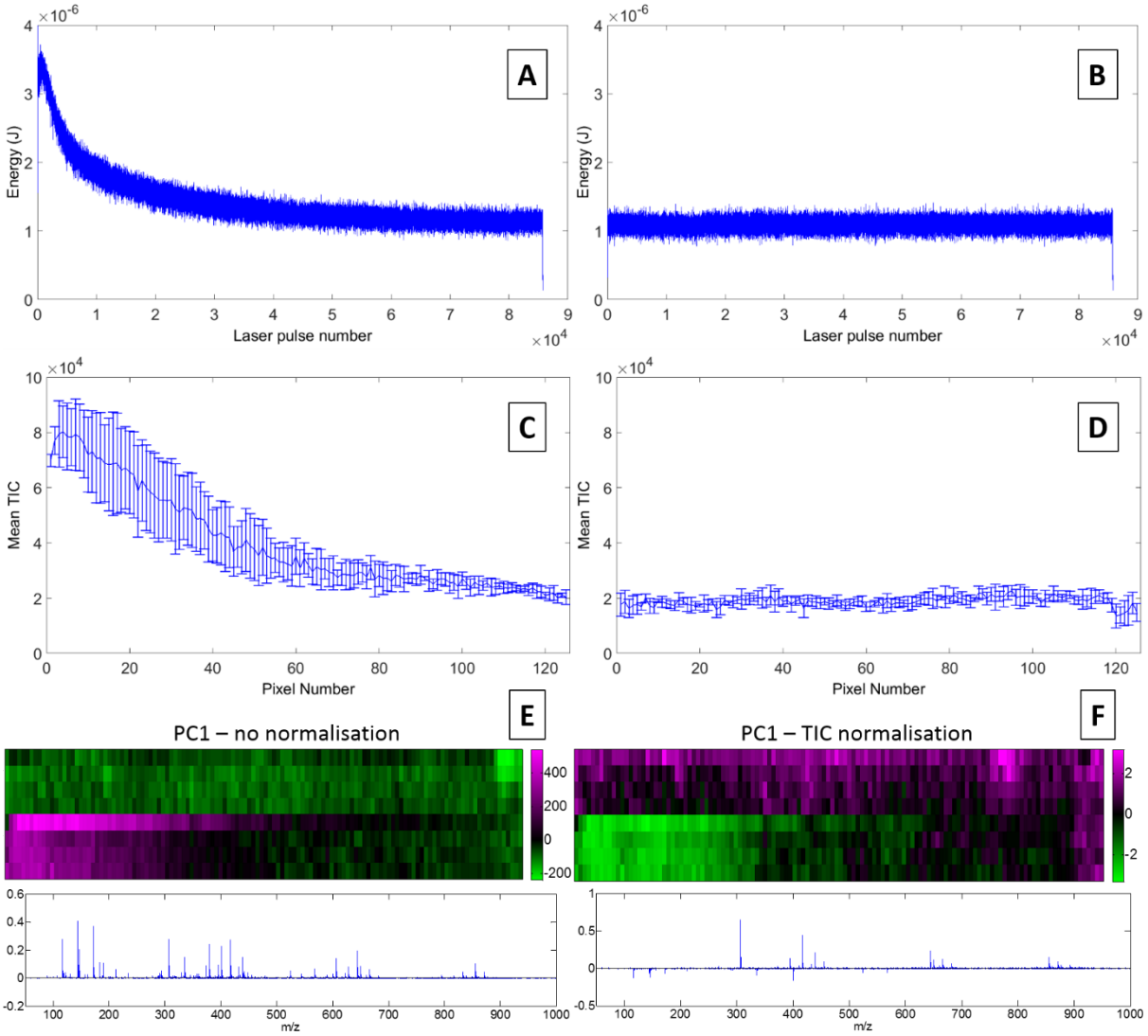

Figure 2. MALDI MSI data acquired from thin film CHCA under two different trigger regimes. Raw single pulse on-line energy measures and mean total ion count (TIC) data for non-shutter (A, C) and shutter (B, D) triggered data respectively. Data derived from principle component analysis of these images is shown for raw (E) and TIC normalized (F) data. The top half of data within the images in E and F were acquired with the shutter and the bottom half without. Significant variation in energy-per-pulse, total-ion-intensity and spectral complexity are evident depending upon the laser triggering method used with the shutter method providing improved stability.

The energy measures from non-shutter-triggered and shutter-triggered data show the considerable increase in initial energy due to some combination of spiking and thermal equilibration type phenomenon within the non-shutter-triggered data (Figure 2 A and B). The values shown have been calibrated to show the value incident upon the sample itself within the ion source. The energy for the non-shutter triggered data only relaxes to the equilibrium operating level of the laser, at the repetition rate used, by the end of raster line. The total ion count (TIC) detected per pixel for the concomitantly acquired MALDI MSI data from the thin layer CHCA sample is displayed as an average ± standard deviation from the four horizontal raster lines acquired (Figure 2 C and D). It is clear that the TIC correlates with the increased energy-per-pulse emitted due the spiking / thermal phenomena caused by the direct triggering of the laser at the beginning of each raster line (Figure 2 C). Whereas, the continuously operated, shutter triggered laser shows a much more stable TIC across the four raster lines (Figure 2 D), giving a value equal to that reached at the end of the line in Figure 2 C throughout the acquisition. Despite the effect of these energy instabilities clearly showing within the TIC data, the effect on the mass spectrometric data is more complex than a global intensity increase across all peaks within the mass spectra, as may be assumed. Principal component analysis (PCA) was carried out on the un-normalised and TIC normalised data to give further insight into the spectral effects of the energy differences afforded by these two triggering setups (Figure 2 E and F). The un-normalised PCA score plot and loading spectrum for component 1 shows what appears to mostly be global intensity changes due to the varying incident energy causing the desorption and ablation from the sample; whereby the top half of the image (where the shutter was employed) correlates with only very minor variation in small scale peaks and the lower half of the image (without shutter and so with considerable energy variation across the image) shows correlation with a substantial change in the

detection of many peaks across the mass spectrum. If linear intensity changes across all peaks in the mass spectrum were the only result of the energy variation resulting from these two trigger setups then TIC normalising prior to carrying out PCA should show the shuttered and non-shuttered pixels to have much more similar scores within the subsequent PCA score plot. These data are shown in Figure 2 F and it is evident within the TIC normalised PC 1 score plot and loadings spectrum is the shuttered and non-shuttered data are still showing substantial differences. Therefore, within these analyses, rather than what look like global intensity differences, there is more complex chemical variation between the two data sets corresponding to a reduced correlation to commonly observed high mass matrix cluster peaks in the non-shutter triggered data. The correlation of changing detected TIC and shifting spectral nature with the reduced energy stability, resulting from the non-shutter based laser triggering method, clearly demonstrate the potential issues which can arise from poor laser stability due to this type of triggering method.

Investigation into the use of a mechanical shutter in MALDI MSI of murine brain tissue

To further study these phenomena and their influence within MALDI MSI the same shutter triggered and non-shutter triggered systems were employed to acquire data from the right hemisphere of each of two coronal serial sections of murine brain tissue coated with CHCA. Images and other analyses from these image datasets are shown in Figure 3.

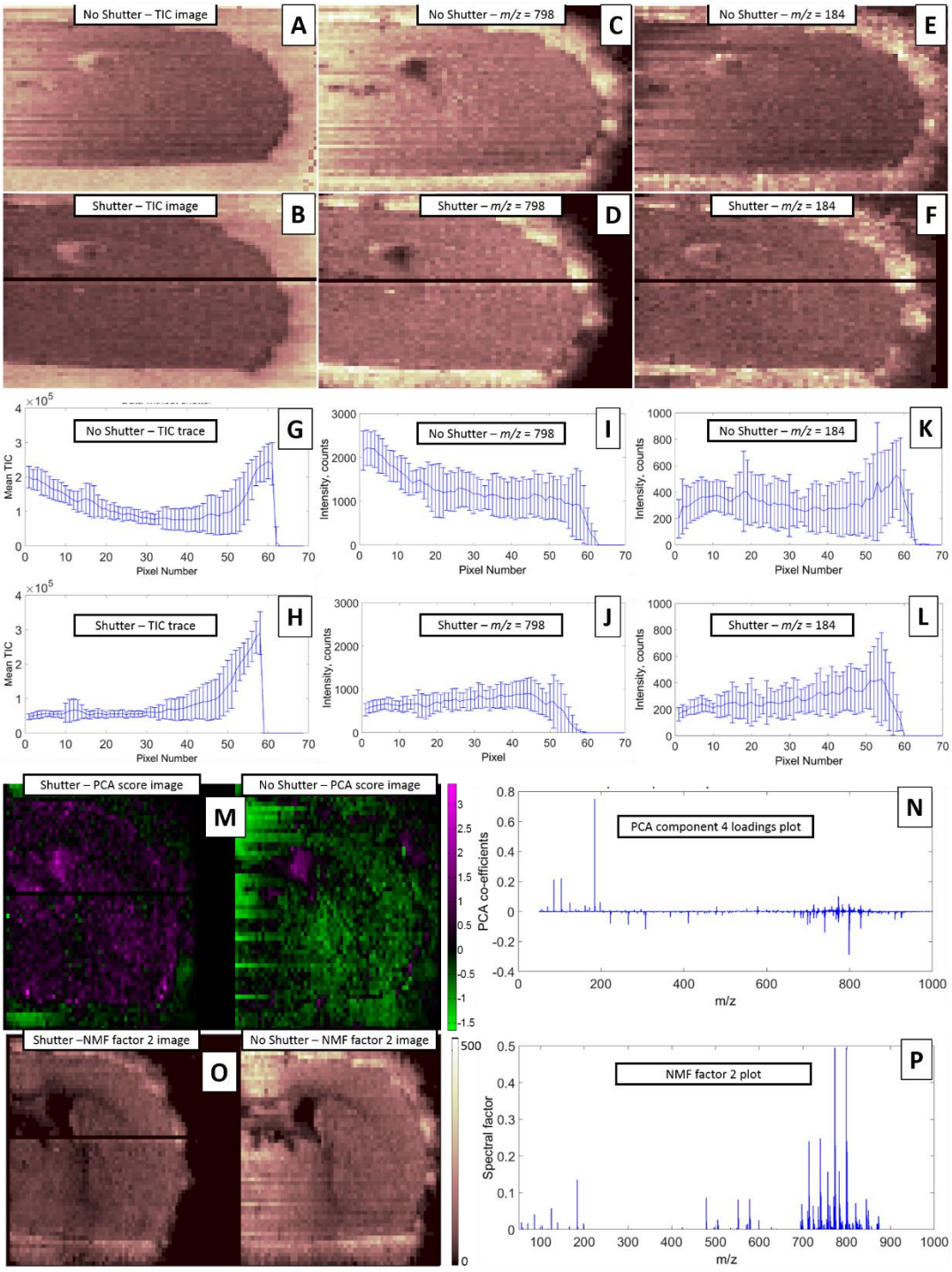

Figure 3. Effect of shutter triggering in tissue MALDI MS imaging. Images of TIC, PC 34:1 $[M+K]^+$ at *m/z* = 798.5 and PC lipid head-group fragment at *m/z* = 184.1 for both shutter triggered and non-shutter triggered data sets are shown in A through F respectively. Images are from region 6 mm wide and 5.5 mm high Corresponding traces for these images showing mean ± standard deviation from each column of pixels in the image are shown in G through L. PCA

and NMF plots are shown in M, N, O and P to help summarise aspects of the spectral changes caused by the differing trigger setups. Images A – F are images taken from regions ~ 6 mm wide and ~ 5.3 mm wide and images within M and O are MVA data from these same images, slightly resized for display purposes.

The energy per pulse of the laser within these tissue imaging experiments followed the same shape and magnitude of trend as displayed in Figure 2 A and B and so are not included here but is displayed in supplementary information (SI) Figures S 1 and S 2. Tissue images acquired with use of the shuttered trigger setup or with the non-shuttered direct triggered setup are displayed for the TIC (Figure 3 A and B), PC 34:1 $[M+K]^+$ (tentatively assigned from literature [14-17]) at *m/z* = 798.5 (Figure 3 C and D) and PC lipid head-group fragment (tentatively assigned from literature [$C_5H_{14}NNaO_4P$] [18, 19]) at *m/z* = 184.1 (Figure 3 E and F). Lipid ion PC 34:1 $[M+K]^+$ at *m/z* = 798.5 was chosen for display here due to its relatively homogenous detection within MALDI MSI of murine tissue [16] meaning it will better exemplify changes in the detected ion intensity within this tissue imaging context. The PC lipid head-group fragment at *m/z* = 184.1 is chosen for display here as fragmentation of detected species within MALDI MS is intimately linked to the incident laser energy.[20] Consequently, the image of this fragment, a fragment from a commonly observed abundant class of lipids, is highly relevant to the study of varying energy in MALDI MSI. In the four single ion images (Figure 3 C – F) there is a clearly visible halo around the tissue section itself resulting from an overly 'wet' matrix deposition, a common feature of solvent based matrix deposition within MALDI MSI. Whilst this does create an obvious undesirable feature within these images it is not problematic for this type of study and can even be taken advantage of when forming

conclusions regarding the changing stability of the laser due to the differing ablation threshold of on-tissue vs. on-plate desorption / ablation behaviors. In all three of these image pairs, the effect of the more stable laser energy resulting from the shutter triggering (Figure 3 B, D and F) and the (initially high) decreasing laser energy resulting from the direct non-shutter triggering (Figure 3 A, C and E), are clear in the more consistent ion intensities across the tissue section seen in Figure 3 B, D and F. In line with the elevated energy at the beginning of each raster line, more intense regions are clear to the left of the TIC and *m/z* = 798.6 images. Interestingly there is a reduction in the intensity of *m/z* = 184.1 resulting from these higher energies which may appear counter intuitive to the idea that increased internal energy results from increased laser energy. However, this appears to be due to these high energies (and so fluences – 293 J/m^2 at the most intense) causing the PC lipid species to fragment into smaller structures than *m/z* 184.1. For example, the tissue images of a smaller component of the PC headgroup detected at *m/z* = 56 do show an increase to the left hand side of the image in accordance with the increased energies of the non-shutter data (SI Figures S 3 and S 4). The increase or decrease of various ion intensities across each raster line in the non-shutter triggered data (from left to right), in response to the decreasing energy per pulse, all show greatest similarity in on-tissue ion intensities to the shutter triggered image in the right most tissue region. This is also the region in which the laser energy finally decreases back to the level set by the attenuator for the equilibrium operation demonstrated in the shutter triggered data set (SI Figure S 1 and S 2). These changes are further demonstrated in the graphs within Figure 3 G through L in which the intensities in each column of the corresponding tissue images are plotted as mean ± standard deviation. Again, the influence of the varying energy is clear in the increased mean ion intensity for the TIC and *m/z* = 798.6 and the decrease in *m/z* = 184.1 to the left of their corresponding non-triggered traces (Figure

3 G, I and K). It also appears that there is less variation in the ion intensity detected within the shutter triggered data (as demonstrated by the smaller error bars) as compared to the corresponding non-shuttered data.

As with the thin-film CHCA investigation MVA were carried out on this tissue imaging data. Both shutter and non-shutter images were combined into a single image prior to MVA. Again PCA was performed and an example loadings plot and score image is shown in Figure 3 M and N. Here component 4 shows the shutter triggered, on-tissue, portion of the image grouping together in a clear and relatively homogenous manner and the off-tissue halo portion of this image correlates with the majority of the non-shutter triggered image, with only some tissue features correlation with those of the shutter image. The corresponding loadings plot clearly shows that these differences are not only due to the intensity differences shown within the single ion analyses (Figure 3 A – L) but result from a more complex change in detected ion intensity across the whole mass spectrum, both within the matrix and lipid fragment dominated regions of low *m/z* and the mostly intact lipid ions above approximately *m/z* = 700. This further demonstrates that varying detected ion intensities, resulting from the non-shutter triggered laser energy decrease across each raster line, are not accounted for by a typical univariate normalization such as TIC normalization, as the changes in chemistry caused by this energy change are complex and variable. In addition to the PCA, non-negative matrix factorisation was also applied to these image data. NMF is often applied within MSI to provide data reduction and chemical interpretation of variance contributions in a way that is similar to PCA but avoids the negative loadings and factors in a way that potentially makes the data easier to interpret [21]. Here the loadings and score plot of the second NMF factor are shown (Figure 3 O and P). The differential weightings of the detected ions within the factor 2 loadings plot (Figure 3 P) may, at first, look like a fairly typical MALDI MSI spectrum from murine brain,

which would lead one to conclude that this factor was describing only global intensity differences. However, when compared to a mean on-tissue mass spectra (SI Figure S 5), considerable differences are evident in the relative intensities of different ions across the *m/z* range. Also, clear within these mean spectra is the increased intensity of the majority of peaks within the non-shutter spectrum. This is due to the high energy of the laser at the beginning of each raster line increasing the detected ion intensity within these regions as shown in Figure 3 A – F. This is also the case for other NMF factors resulting from this analysis (SI Figure S 6). The corresponding NMF factor 2 image (Figure 3 O) shows the correlation with the *m/z* loadings shown in Figure 3 P as being relatively even across the tissue spectrum, for the shuttered data, as compared to the intense correlation with these factors to the left of the non-shuttered NMF image, which fades to an intensity similar to that of the shutter triggered data to the right hand side of the tissue. This is similar to the intensity variations seen in the single ion images, where the detected intensity in the non-shutter triggered data reduces to the level of the shutter triggered data to the right hand side of the image, in line with the reducing energy per pulse (SI Figures S 1 and S 2), as the laser equilibrates over the course of each raster line acquisition. These NMF factor loadings and image plots further demonstrate the complexity of the spectral variations across the non-shuttered image due to this changing energy per pulse.

The relationship between detected ion intensity and laser energy or fluence has been studied a number of times by different groups.[1, 7, 13, 22-24]. Within a given fluence range the ion intensity, *I*, is observed to increase according to the power law relationship $I \propto H^m$ where *H* is the fluence and *m* is the fitting parameter. Beyond this exponential like increase there will be a plateau in the detected ion intensity and further increase in fluence will not lead to further increase in detected ions and may even lead to a decrease. This relationship clearly explains

the increase in ion intensity observed in correlation with the increased energy per pulse within the non-shutter triggered data sets within this study and reaffirms the need for stable laser energy within MALDI MS and MSI experiments. What is not obvious from the literature and remains a topic ripe for further study, is the effect of laser energy within more complex systems such as tissue imaging studies. The results here suggest that aside from the anticipated variation in ion intensity with laser energy there are more complex phenomena occurring, where relative amounts of different intact lipid species are detected and differing levels of fragmentation seen depending upon the incident laser energy.

Conclusions

The detected ion intensity was observed to vary due to energy 'spiking' and temperature equilibration type effects when triggering the laser directly from the function generator. These effects can be removed by continuous triggering of the laser in conjunction with a separate mechanical shutter system being used to 'trigger' the laser for mass spectrometric analysis. This allows the laser to operate continuously at equilibrium, even where no MS data is being acquired, ensuring the emitted pulse to pulse energy is stable when the MALDI MS analyses are carried out. The shutter system used here provides a cheap and easy to install solution to non-equilibrium operation laser stability issues, which may be encountered by MALDI MS researchers and practitioners.

The consequence of energy variation as a result of non-equilibrium laser operation demonstrated here is not only observed to cause differences in detected ion intensity for single ions, but also to result in differing relative abundances of detected lipid ions and their characteristic fragments. Commercial MALDI MS systems to not provide for true laser energy

control and monitoring, making knowledge of the behavior of one's laser system difficult to obtain. It is therefore recommended that researchers within MALDI MS and MSI are aware of the behavior of their laser system under different operational conditions, in order to best adjust or account for any laser energy drift due to spiking and short term thermal control effects such as those observed here, or due to longer term drifts in energy due to thermal changes in the lab or damage within the laser optics. A shutter system or other compensatory attenuation feedback setup is recommended for systems in which these phenomena are likely to occur.

Acknowledgments

Thank you to Keith Oakes for very helpful discussion. Funding was provided by NPL strategic research program 'NiCE MSI' (project 116301) and Innovate UK (formerly TSB) award 101788. AD is in receipt of an EPSRC studentship via the PSIBS doctoral training centre (EP/F50053X/1), in collaboration with AstraZeneca and the National Physical Laboratory.

References

1. K. Dreisewerd, The desorption process in MALDI, Chem Rev. **103** (2003) 395-425.
2. J.I. Berry, S. Sun, Y. Dou, A. Wucher, N. Winograd, Laser desorption and imaging of proteins from ice via UV femtosecond laser pulses, Analytical chemistry. **75** (2003) 5146-5151.
3. C.L. Kalcic, G.E. Reid, V.V. Lozovoy, M. Dantus, Mechanism elucidation for nonstochastic femtosecond laser-induced ionization/dissociation: From amino acids to peptides, The Journal of Physical Chemistry A. **116** (2012) 2764-2774.
4. J.A. Bradshaw, O.S. Ovchinnikova, K.A. Meyer, D.E. Goeringer, Combined chemical and topographic imaging at atmospheric pressure via microprobe laser desorption/ionization mass spectrometry–atomic force microscopy, Rapid Commun Mass Sp. **23** (2009) 3781-3786.
5. J.T. Westheide, J.S. Becker, R. Jäger, H.-J. Dietze, J.A. Broekaert, Analysis of ceramic layers for solid oxide fuel cells by laser ablation inductively coupled plasma mass spectroscopy, Journal of Analytical Atomic Spectrometry. **11** (1996) 661-666.
6. A. Zavalin, E.M. Todd, P.D. Rawhouser, J. Yang, J.L. Norris, R.M. Caprioli, Direct imaging of single cells and tissue at sub-cellular spatial resolution using transmission geometry MALDI MS, J Mass Spectrom. **47** (2012) 1473-1481.
7. G. Westmacott, W. Ens, F. Hillenkamp, K. Dreisewerd, M. Schurenberg, The influence of laser fluence on ion yield in matrix-assisted laser desorption ionization mass spectrometry, Int J Mass Spectrom. **221** (2002) 67-81.
8. C. Hollands, The Animals (scientific procedures) Act 1986, The Lancet. **328** (1986) 32-33.

9. R.T. Steven, A.D. Palmer, J. Bunch, Fluorometric Beam Profiling of UV MALDI Lasers, J Am Soc Mass Spectr. **24** (2013) 1146-1152.
10. A.M. Race, I.B. Styles, J. Bunch, Inclusive sharing of mass spectrometry imaging data requires a converter for all, Journal of Proteomics. **75** (2012) 5111-5112.
11. A.M. Race, J. Bunch, Optimisation of colour schemes to accurately display mass spectrometry imaging data based on human colour perception, Anal Bioanal Chem. **407** (2015) 2047-2054.
12. A.M. Race, R.T. Steven, A.D. Palmer, I.B. Styles, J. Bunch, Memory Efficient Principal Component Analysis for the Dimensionality Reduction of Large Mass Spectrometry Imaging Data Sets, Anal Chem. **85** (2013) 3071-3078.
13. S. Guenther, M. Koestler, O. Schulz, B. Spengler, Laser spot size and laser power dependence of ion formation in high resolution MALDI imaging, Int J Mass Spectrom. **294** (2010) 7-15.
14. S.N. Jackson, M. Ugarov, J.D. Post, T. Egan, D. Langlais, J.A. Schultz, et al., A study of phospholipids by ion mobility TOFMS, J Am Soc Mass Spectr. **19** (2008) 1655-1662.
15. H.Y.J. Wang, C.B. Liu, H.W. Wu, J.S. Kuo, Direct profiling of phospholipids and lysophospholipids in rat brain sections after ischemic stroke, Rapid Commun Mass Sp. **24** (2010) 2057-2064.
16. R.T. Steven, A.M. Race, J. Bunch, Para-Nitroaniline is a promising matrix for MALDI-MS imaging on intermediate pressure MS systems, J Am Soc Mass Spectr. **24** (2013) 801-804.
17. K. Shrivas, T. Hayasaka, N. Goto-Inoue, Y. Sugiura, N. Zaima, M. Setou, Ionic matrix for enhanced MALDI imaging mass spectrometry for identification of phospholipids in mouse liver and cerebellum tissue sections, Anal Chem. **82** (2010) 8800-8806.
18. K.A. Zemski Berry, J.A. Hankin, R.M. Barkley, J.M. Spraggins, R.M. Caprioli, R.C. Murphy, MALDI Imaging of Lipid Biochemistry in Tissues by Mass Spectrometry, Chem Rev. **111** (2011) 6491-6512.
19. X. Wang, J. Han, A. Chou, J. Yang, J. Pan, C.H. Borchers, Hydroxyflavones as a New Family of Matrices for MALDI Tissue Imaging, Anal Chem. **85** (2013) 7566-7573.
20. G. Luo, I. Marginean, A. Vertes, Internal energy of ions generated by matrix-assisted laser desorption/ionization, Anal Chem. **74** (2002) 6185-6190.
21. E.A. Jones, A. van Remoortere, R.J. van Zeijl, P.C. Hogendoorn, J.V. Bovée, A.M. Deelder, et al., Multiple statistical analysis techniques corroborate intratumor heterogeneity in imaging mass spectrometry datasets of myxofibrosarcoma, PLoS One. **6** (2011) e24913.
22. J. Soltwisch, T.W. Jaskolla, K. Dreisewerd, Color Matters—Material Ejection and Ion Yields in UV-MALDI Mass Spectrometry as a Function of Laser Wavelength and Laser Fluence, J Am Soc Mass Spectr. **24** (2013) 1477-1488.
23. K. Dreisewerd, M. Schurenberg, M. Karas, F. Hillenkamp, Influence of the Laser Intensity and Spot Size on the Desorption of Molecules and Ions in Matrix-Assisted Laser-Desorption Ionization with a Uniform Beam Profile, Int J Mass Spectrom. **141** (1995) 127-148.
24. H. Qiao, V. Spicer, W. Ens, The effect of laser profile, fluence, and spot size on sensitivity in orthogonal-injection matrix-assisted laser desorption/ionization time-of-flight mass spectrometry, Rapid Commun Mass Sp. **22** (2008) 2779-2790.